The Plant Cell, Vol. 11, 809–824, May 1999, www.plantcell.org © 1999 American Society of Plant Physiologists

Three-Dimensional Microscopy of the Rad51 Recombination Protein during Meiotic Prophase

Amie E. Franklin,[a,1] John McElver,[b] Ivana Sunjevaric,[c] Rodney Rothstein,[c] Ben Bowen,[d] and W. Zacheus Cande[a]

[a] Department of Molecular and Cell Biology, University of California at Berkeley, Berkeley, California 94720
[b] Novartis Agribusiness Biotechnology Research Inc., 3054 Cornwallis Road, Research Triangle Park, North Carolina 27709
[c] Department of Genetics and Development, College of Physicians and Surgeons, Columbia University, New York, New York 10032-2704
[d] Lynx Therapeutics, Inc., Hayward, California 94545

An open question in meiosis is whether the Rad51 recombination protein functions solely in meiotic recombination or whether it is also involved in the chromosome homology search. To address this question, we have performed three-dimensional high-resolution immunofluorescence microscopy to visualize native Rad51 structures in maize male meiocytes. Maize has two closely related *RAD51* genes that are expressed at low levels in differentiated tissues and at higher levels in mitotic and meiotic tissues. Cells and nuclei were specially fixed and embedded in polyacrylamide to maintain both native chromosome structure and the three dimensionality of the specimens. Analysis of Rad51 in maize meiocytes revealed that when chromosomes condense during leptotene, Rad51 is diffuse within the nucleus. Rad51 foci form on the chromosomes at the beginning of zygotene and rise to ~500 per nucleus by mid-zygotene when chromosomes are pairing and synapsing. During chromosome pairing, we consistently found two contiguous Rad51 foci on paired chromosomes. These paired foci may identify the sites where DNA sequence homology is being compared. During pachytene, the number of Rad51 foci drops to seven to 22 per nucleus. This higher number corresponds approximately to the number of chiasmata in maize meiosis. These observations are consistent with a role for Rad51 in the homology search phase of chromosome pairing in addition to its known role in meiotic recombination.

INTRODUCTION

Meiosis results in halving the chromosome complement, a process that is required for the formation of haploid gametes or cells. This involves a complex orchestration of events, including large-scale chromosome remodeling and movement within the nucleus. Cytological analysis of meiosis has revealed that the distinctive stages of meiotic prophase (leptotene, zygotene, pachytene, diplotene, and diakinesis) can be found in the plant, animal, and fungal kingdoms (John, 1990; Roeder, 1995). During leptotene, chromosomes condense, and the axial elements of the synaptonemal complex (SC) are assembled onto the chromosomes. During zygotene, homologous chromosomes synapse as defined by the installation of the central element of the SC (Moses, 1956). The beginning of zygotene is distinguished by the de novo formation of the telomere bouquet (Scherthan et al., 1996; Bass et al., 1997). The telomere bouquet is a conspicuous nuclear arrangement in which all of the telomeres are clustered together on the nuclear envelope (Dernburg et al., 1995). This arrangement may aid in pairing by coorienting the chromosomes (Gillies, 1975; Bass et al., 1997). By pachytene, chromosomes are synapsed along their entire length, and meiotic recombination is completed (Padmore et al., 1991). Finally, in diplotene, the SC disassembles, and the chiasmata responsible for holding the homologs together become cytologically evident (Creighton and McClintock, 1931; Stern, 1931).

Proteins involved in homologous recombination are expressed during meiosis. The Rad51 recombination protein and its meiotic-specific homolog Dmc1 were first discovered in *Saccharomyces cerevisiae* (Bishop et al., 1992; Shinohara et al., 1992). Rad51 is homologous to the bacterial RecA protein, which is responsible for DNA strand exchange, suggesting that Rad51 may have a similar function in eukaryotic cells (Shinohara et al., 1992). Subsequently, Rad51 homologs were identified in a number of different eukaryotes (Cheng et al., 1993; Morita et al., 1993; Shinohara et al., 1993). In *S. cerevisiae*, Rad51 is required for many

[1] To whom correspondence should be addressed. E-mail franklin@candelab.berkeley.edu; fax 510-643-6791.

mitotic homologous recombination events, and both Rad51 and Dmc1 are required for meiotic homologous recombination (Smith and Nicholas, 1998). In vitro biochemical studies indicate that Rad51 proteins by themselves are capable of catalyzing homologous DNA strand exchange (Sung and Robberson, 1995; Baumann et al., 1996; Maeshima et al., 1996; Gupta et al., 1997). The efficiency and specificity of this reaction are improved significantly when both Rad52 and replication protein A proteins are added (Sung, 1997; Benson et al., 1998; New et al., 1998; Shinohara and Ogawa, 1998). However, it is likely that other proteins also participate in forming the meiotic recombination complex in vivo because the electron-dense nodules thought to be responsible for recombination are on the order of 100 nm in diameter (Carpenter, 1975; Hobolth, 1981). Rad51 has been demonstrated to be a component of some of the early recombination nodules by immunoelectron microscopy (Anderson et al., 1997; Moens et al., 1997).

Rad51 has an established role in meiotic recombination; however, the presence of large numbers of discrete Rad51 foci during chromosome synapsis has led to the suggestion that it may perform a second function during meiotic prophase. Rad51 and Dmc1 proteins have been immunolocalized to unsynapsed and partially synapsed SCs or chromosomes in lily, mice, and humans (Ashley et al., 1995; Terasawa et al., 1995; Barlow et al., 1997). These data have been interpreted in light of two conflicting models; either Rad51 is required for the chromosome homology search leading to synapsis independent of any role in meiotic recombination, or Rad51 is initiating meiotic recombination, which, in turn, is required for synapsis. In support of the first model, Ashley et al. (1995) claimed that Rad51 foci spaced along the length of the SC cores fuse together for homology search and synapsis. However, Barlow et al. (1997) interpreted these foci as early recombination complexes that ultimately yield mature meiotic recombination complexes upon synapsis (Barlow et al., 1997). Because it is not clear when the chromosome homology search is being performed in these organisms, either model may be valid.

To compare Rad51 behavior directly with nuclear and chromosome structure during meiosis, we have used the maize male meiocyte as a model system for studying the molecular cytology of meiosis. We have developed a procedure that maintains both native chromatin structure and the three-dimensional structure of meiotic nuclei to visualize native Rad51 complexes. Furthermore, we have used optical sectioning microscopy combined with mathematical deconvolution of the optical data that replaces the out-of-focus light to its original focal plane (Chen et al., 1995). The initial goal of this study was to determine the precise kinetics of Rad51 appearance with respect to formation of the telomere bouquet. Microscopical analysis of nuclear spreads has not addressed this particular question, and the three-dimensional immunofluorescence approach presented here extends and complements the previous studies of Rad51 behavior.

For this study, we have cloned cDNAs encoding two maize Rad51 homologs and developed a generally usable three-dimensional immunofluorescence procedure for localizing Rad51 and other nuclear and cellular proteins. Our analysis reveals that in maize meiocytes, the initial appearance of Rad51 foci on chromosomes coincides with the formation of the telomere bouquet at the transition between the leptotene and zygotene stages. By mid-zygotene, the numbers of Rad51 foci peak at ~500 per nucleus and are clearly associated with unpaired and partially paired chromosomes, which is consistent with a role for Rad51 in chromosome pairing. Paired contiguous Rad51 foci are evident on paired chromosomes and may be sites at which chromosome homology actually is being compared. By pachytene, the number of Rad51 foci decreases to seven to 22 per nucleus, which is consistent with the expected number of meiotic recombination events. These observations support a role for Rad51 in mediating chromosome homology search in zygotene and a later role during chromosome crossing-over in pachytene.

RESULTS

Maize Has Two Closely Related *RAD51* Genes

Two full-length clones with marked similarity to eukaryotic Rad51 gene products were isolated from a maize tassel cDNA library. *ZmRAD51a* and *ZmRAD51b* encode closely related 340–amino acid polypeptides (Figure 1A), with almost all of the amino acid differences present at the N termini. ZmRad51a and ZmRad51b are 90% identical to each other and are 69 and 70% identical to human Rad51, respectively. Both maize Rad51 proteins clearly fall within the Rad51 subfamily rather than the Dmc1/Lim15 subfamily of RecA-related proteins (Figure1B). The *ZmRAD51a* and *ZmRAD51b* clones map to separate locations in the maize genome, indicating that the two cDNAs are derived from independent loci. *ZmRAD51a* was mapped to chromosome 7, bin 7.04, and *ZmRAD51b* was mapped to chromosome 3, bin 3.04 to 3.06. In addition to the two *RAD51*-related genes reported here, independent work has shown that maize has two genes closely related to yeast *DMC1* (S. Tabata, personal communication; J. McElver and B. Bowen, unpublished data).

To examine the tissue specificity of *ZmRAD51* gene expression, we performed RNA gel blot analysis with mRNA from different maize tissues. Probes derived from the 3′ untranslated regions of both *RAD51* genes identified bands of ~1.4 kb in every tissue analyzed but at varying expression levels, compared with the constituitively expressed *DAD1* gene (defender against cell death), which is homologous to the *S. cerevisiae* oligosaccharyl-transferase *OST2* gene (Figure 1C; J. McElver and B. Bowen, unpublished data). Generally, *ZmRAD51b* was expressed at levels lower than

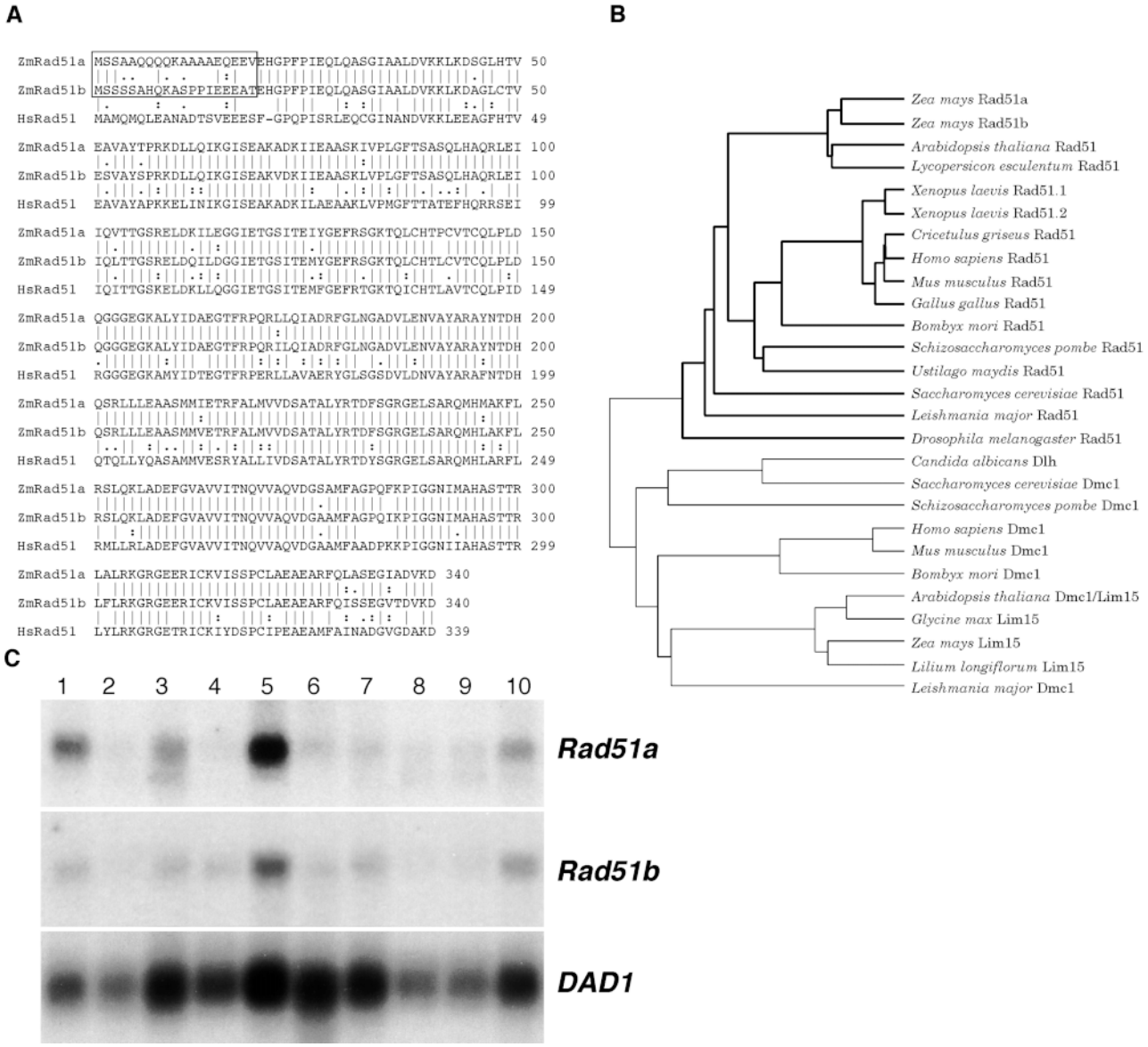

Figure 1. Maize Rad51 Sequences and Expression.

(A) Alignment of the deduced primary amino acid sequences of ZmRad51a, ZmRad51b, and HsRad51. Bars indicate identical amino acids, colons indicate highly conserved amino acids, and single dots indicate less conserved amino acids. The first 19 residues (boxed) account for most of the sequence differences between the maize proteins. The maize sequence data are available from GenBank under accession numbers AF079428 and AF079429.

(B) Cladogram of a representative set of Rad51/Dmc1 proteins, indicating the relative relatedness of ZmRad51 homologs. The thicker lines indicate the Rad51 group, and the thinner lines indicate the Dmc1 group. The cladogram was calculated using the Genetics Computer Group Pileup program (Genetics Computer Group, Madison, WI) with default parameters. Sequence identification numbers from the Entrez peptide database for the proteins are given from Arabidopsis (third) to *Leishmania major* (bottom), excluding *Zea mays* Lim 15, and are as follows: 1706947, 2500107, 2500105, 2500106, 2500103, 548663, 585772, 585770, 2058709, 548664, 2500102, 131783, 3132709, 2500104, 1706446, 118683, 2696694, 2135607, 2500100, 2058711, 1790922, 1518157, 585771, and 3132711. The maize Lim15 homolog sequence was provided courtesy of S. Tabata (personal communication).

(C) Expression of *ZmRAD51* genes in maize tissues. The top blot was probed with the 3′ untranslated region of *ZmRAD51a*; the central blot is the same blot reprobed with the 3′ untranslated region of *ZmRAD51b.* The lower blot is the same blot reprobed with the constituitively expressed maize *ZmDAD1* gene (J. McElver and B. Bowen, unpublished data). Lane 1, meiotic prophase tassel; lane 2, meiotic tassel; lane 3, tassel with tetrads/uninucleate pollen; lane 4, shedding tassel with mature pollen; lane 5; meiotic ears (2.8 to 4.8 cm); lane 6, mature ear (11.8 cm); lane 7, embryos 7 days after pollination; lane 8, embryos 21 days after pollination; lane 9, seedling leaves; and lane 10, seedling roots. $OD_{260\ nm}$ was used to estimate the total amount of poly(A)-enriched RNA loaded per lane: lanes 1 to 4 contain 1.7 μg, lanes 5 to 8 contain 3.7 μg, and lanes 9 and 10 contain 2.5 μg.

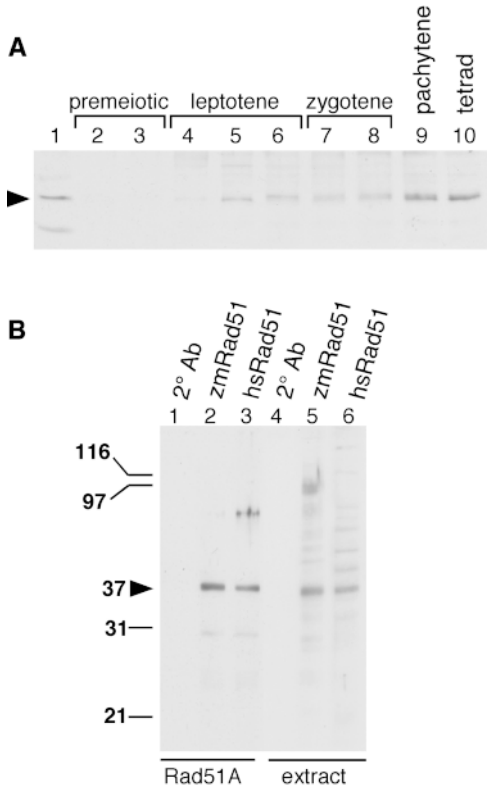

Figure 2. Rad51 Protein Accumulates during Meiosis.

(A) Immunoblot of staged maize A344 anthers (three per lane) probed with anti-ZmRad51a antibody. Lane 1 contains 1 ng of bacterially expressed ZmRad51a protein; lane 2, 0.6-mm premeiotic anthers; lane 3, 0.8-mm premeiotic anthers; lane 4, 1.0-mm leptotene anthers; lane 5, 1.2-mm leptotene anthers; lane 6, 1.5-mm leptotene anthers; lane 7, 1.8-mm zygotene anthers; lane 8, 2.0-mm zygotene anthers; lane 9, 2.5-mm pachytene anthers; and lane 10, 3.0-mm tetrad stage anthers (two anthers). Arrowhead indicates the position of Rad51.

(B) Comparison of the specificity of the anti-ZmRad51a antibody and the anti-HsRad51 antibodies. Lanes 1 to 3 contain pure maize Rad51a protein probed with secondary antibodies (2° Ab) alone, anti-ZmRad51a antibodies, and anti-HsRad51 antibodies, respectively. Lanes 4 to 6 contain meiotic tassel extract probed with secondary antibodies alone, anti-ZmRad51a antibodies, and anti-HsRad51 antibodies, respectively. Molecular mass markers are given at left in kD. Arrowhead indicates the position of Rad51.

ZmRAD51a but with the same tissue specificity. Highest levels of message were present in reproductive tissues containing cells undergoing early stages of meiosis, for example, developing tassels and ears (Figure 1C, lanes 1 and 5). Significant expression also was seen in tassels containing predominantly quartet/uninucleate-stage pollen grains undergoing postmeiotic mitoses (lane 3) and in seedling root tissue that is rich in mitotically active meristematic cells (lane 10). Lower levels of expression generally were seen in tissues containing fewer actively dividing cells, for example, kernels, seedling leaf, and mature tassel or ear.

Rad51 Protein Primarily Accumulates during Mid-Leptotene

To determine whether the Rad51 protein was present during meiotic prophase, we probed total protein from sequentially staged anthers with polyclonal antibodies made against the bacterially expressed ZmRad51a fusion protein. These antibodies recognize both ZmRad51a and ZmRad51b proteins (data not shown). Rad51 protein levels barely were detectable before meiosis (Figure 2A, lanes 2 and 3), increased significantly during mid-leptotene (lane 4), and then continued to rise during zygotene and remained at high levels through the pachytene and tetrad stages (further stages

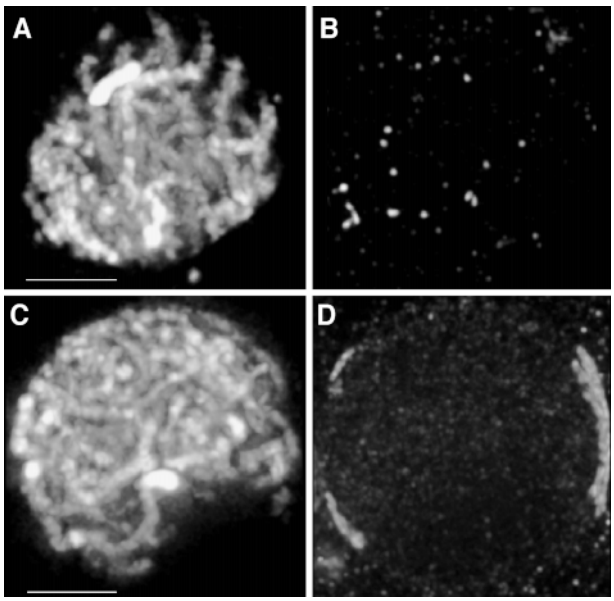

Figure 3. Specificity of the Anti-HsRad51 Antibodies for Maize Rad51 Epitopes.

Bright nuclear foci disappeared when anti-HsRad51 antibodies were preincubated with ZmRad51a-containing extract. Eight-micron deep projections (24 optical sections) of two mid-zygotene nuclei are presented.

(A) and **(B)** Mid-zygotene nucleus stained for DNA with DAPI and immunostained with anti-HsRad51 antibodies preincubated with control extract.

(C) and **(D)** Mid-zygotene nucleus stained for DNA with DAPI and immunostained with anti-HsRad51 antibodies preincubated with ZmRad51a-containing extract. Slides containing both nuclei were processed at the same time, had nearly identical DAPI-staining intensities, and were scaled identically.

Bars in **(A)** and **(C)** = 5 μm for **(A)** to **(D)**.

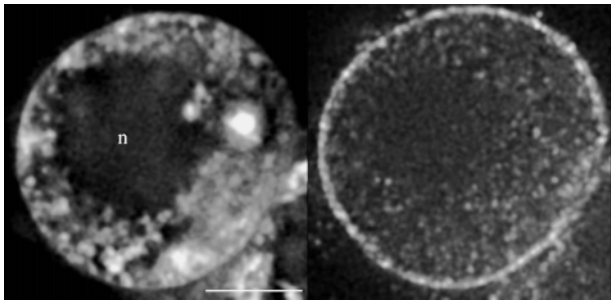

Figure 4. Rad51 Is Diffuse in Nuclei at the Leptotene Stage.

Shown are projections (0.9 μm deep; three optical sections) of a representative leptotene nucleus. The left panel shows the DNA stained with DAPI. The central unstained area is the nucleolus (n). The right panel shows the same nucleus stained with anti-HsRad51 antibodies. Bar = 5 μm.

were not tested). The increase in Rad51 protein probably reflects the increase in the amount of Rad51 protein per cell during meiotic prophase because the ~100 meiocytes per anther undergo meiosis synchronously (Staiger and Cande, 1993).

Native Rad51 Structures Can Be Immunostained

We have developed a three-dimensional immunofluorescence procedure to analyze the subcellular distribution of Rad51 during meiosis. Native chromosome structure was maintained by fixing with a special buffer (Dawe et al., 1994), and whole cells or nuclei were embedded in a 5% polyacrylamide gel to maintain their three-dimensional structure (Bass et al., 1997). We were able to immunostain these cells for Rad51, indicating that chromatin and protein structure do not have to be denatured to visualize DNA binding proteins. Furthermore, this technique generally is usable and has been used subsequently to visualize a number of other nuclear and cellular proteins.

To visualize Rad51 in maize nuclei, we used antibodies generated against the human HsRad51 protein because the ZmRad51 antibodies do not recognize the native protein in situ. These same anti-HsRad51 antibodies were used by Terasawa et al. (1995) to visualize Rad51 in lily meiocytes, who used a second antibody to visualize the closely related protein Lim15, the lily Dmc1 homolog. We confirmed that the anti-HsRad51 antibodies recognized maize Rad51 proteins by protein gel blot analysis and by immunofluorescence. The anti-HsRad51 antibodies probably recognized both ZmRad51a and ZmRad51b proteins because they are nearly 100% identical to each other in the region that is most similar to HsRad51 (Figure 1A). On protein gel blots, the anti-HsRad51 antibodies, like the anti-ZmRad51 antibodies, specifically recognized the bacterially expressed fusion protein His_6-ZmRad51a and a major 37-kD protein in meiotic tassel extracts that corresponds to the size of both maize Rad51 proteins (Figure 2B). Minor protein bands also were recognized by the polyclonal antiserum; consequently, we confirmed the specificity of the antibodies by immunodepletion, as described below.

Immunofluorescence with the anti-HsRad51 antibodies on meiocytes midway through meiotic prophase (zygotene) revealed the presence of bright nuclear-localized foci (Figure 3B, control treatment). Immunodepletion of the anti-HsRad51 antibodies by preincubation with extracts containing ZmRad51a protein eliminated the bright nuclear foci (Figure 3D), indicating that these foci contain Rad51 epitopes. Protein gel blot analysis confirmed that the treated antibodies, but not the control-treated antibodies, were depleted of Rad51-specific antibodies (data not shown). Weak staining of the nuclear envelope was persistent, even with the treated antibodies (Figure 3D); however, because the staining was extranuclear, it did not interfere with our analysis.

The Rad51 Protein Is Diffuse When Chromosomes Are Condensing

Immunofluorescence microscopy with the HsRad51 antibodies on leptotene-staged nuclei revealed diffuse Rad51 staining and a few weak Rad51 foci (Figures 4 and 5, and Table 1). Leptotene meiocytes were easily identified because they have a single, large, centrally located nucleolus. Furthermore, partially condensing strands of the leptotene chromosomes were apparent throughout the nucleus. Occasionally, a few Rad51 foci just two to three times brighter than this diffuse signal were present. The nuclear envelope also had some bright-staining foci, which may represent either new Rad51 protein being imported into the nucleus or the nonspecific staining described previously.

Table 1. Number of Rad51 Foci and Rad51 Pairs during Meiotic Prophase

Stage	Range Rad51	Mean ±SD, Median	Range Rad51 Pairs	*n*[a]
Premeiotic	0	0	0	1
Leptotene	0 to 6	1 ± 2.0	1	5
Early zygotene	34 to 226	163 ± 67, 155	0 to 15	5
Mid-zygotene	370 to 668	493 ± 79, 505	14 to 50	10
Late zygotene	28 to 62	47 ± 13, 49	5 to 11	5
Pachytene	7 to 22	15 ± 5, 16	0 to 5	8
Diplotene	0	0	0	4
Nonmeiotic[b]	0	0	0	2

[a] *n*, number of nuclei analyzed.
[b] Tapetal nuclei.

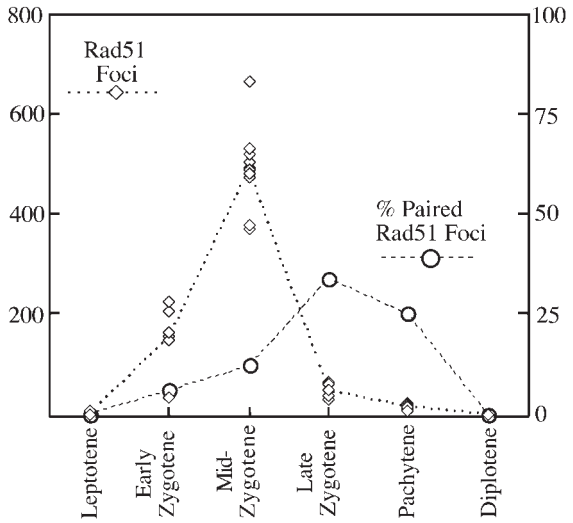

Figure 5. Stage-Specific Numbers of Rad51 Foci during Meiosis.

Number of Rad51 foci per nucleus (left y axis) during meiotic prophase stages (x axis). Individual data points for each nucleus are represented as diamonds, and the dashed line shows the average number of Rad51 foci per nucleus per stage (right y axis). The circles represent the average proportion of Rad51 foci present as paired foci (dotted line).

Rad51 Foci Appear When Chromosomes Are Pairing

Large numbers of bright Rad51 foci were observed in zygotene-staged nuclei (Figures 5 and 6A to 6D, and Table 1). We used the displacement of the nucleolus from the center to the edge of the nucleus to identify cells in zygotene because it is a sensitive indicator for the formation of the telomere bouquet, which is initiated at the beginning of zygotene (Bass et al., 1997). The nucleolus-organizing region DNA is adjacent to the telomere on chromosome 6 and becomes associated with the nuclear envelope when the telomeres bind to the nuclear envelope and then cluster together. The nucleus in Figure 6A with a total of 34 Rad51 foci on its unpaired chromosomes is a rare example of a leptotene-to-zygotene transition nucleus. In this nucleus, the telomere bouquet has formed, as evidenced by the coaligned chromosomes at the base of the nucleus; however, the nucleolus with its associated telomeres is opposite the bouquet. The telomere associated with the nucleolus is always the last to reach the telomere bouquet due to steric hindrance of the nucleolus itself. The Rad51 foci in this transition nucleus were brighter than the diffuse nuclear staining seen in leptotene (Figure 4). As shown in the three-dimensional model for this nucleus (Figure 6E), the Rad51 foci appear to be excluded from the nucleolus but are distributed throughout the remaining nuclear volume. There does not appear to be any specific clustering of the Rad51 foci near the telomere bouquet. An early zygotene nucleus, shown in Figure 6B, has 226 Rad51 foci that also appear randomly distributed throughout the nucleus. Neither of the nuclei shown in Figures 6A or 6B have undergone the chromatin remodeling associated with prezygotene, as exemplified by the uncoiling of the heterochromatic knobs (Dawe et al., 1994). These observations suggest that the appearance of Rad51 foci on the chromosomes does not require this remodeling event. Because prezygotene structural changes are closely associated with the initiation of synapsis, these data do not exclude the possibility that chromatin remodeling is important for other aspects of the homology search and/or synapsis.

By the middle of zygotene, the number of Rad51 foci reached their peak, ranging from 370 to 668 per nucleus (Figure 5 and Table 1). These Rad51 foci were distributed primarily on unpaired or partly paired chromosomes, as shown in the nucleus in Figure 6C. The region containing paired chromosomes at the top of this nucleus was essentially free of Rad51 foci, whereas most of the foci were distributed over the central portion of the nucleus, where there was partial pairing. By late zygotene, when almost all of the chromosomes were completely paired, the numbers of Rad51 foci dropped dramatically, ranging from 28 to 62 foci per nucleus (Figure 6D).

Paired Rad51 Foci Appear on Paired Chromosomes during Zygotene

Throughout zygotene, a consistent feature we observed was the presence of two adjacent or contiguous Rad51 foci on paired chromosomes (Figures 5 and 7, and Table 1). This was particularly striking in late zygotene, when these structures represented on average 34% of the total Rad51 foci. In one cell, 50% of the foci were paired (Figure 6D; 36 Rad51 foci and nine Rad51 pairs). The paired Rad51 foci were evident in both the original raw data and in the deconvolved data (data not shown) and thus are not an artifact of mathematical deconvolution. Although the peak intensities of the two adjacent Rad51 foci were often centered over the chromosome axes, the Rad51 signal was continuous but lower in intensity between the chromosomes. The distance between the peak intensities of the two Rad51 foci were on average 0.46 $\pm$ 0.13 μm apart (peak-to-peak intensity: range 0.24 to 0.79 μm; $n = 34$). For comparison, the width of the SC in maize is $\sim$0.18 to 0.20 μm (Maguire et al., 1993), whereas the center-to-center distance of synapsed chromosomes is $\sim$0.42 μm. Often the intensity of one of the two foci was significantly brighter than its partner. For example, in Figure 7E, the upper Rad51 signal is twice as bright as the lower signal. In Figure 7F, the Rad51 structure is bar shaped instead of having two associated foci. In Figures 7G and 7H, even more striking examples of paired Rad51 foci are present. There are three sequential sets of Rad51 foci on a pair of coaligned chromosomes. The first Rad51 signal is comma shaped, the second Rad51 signal appears bilobed,

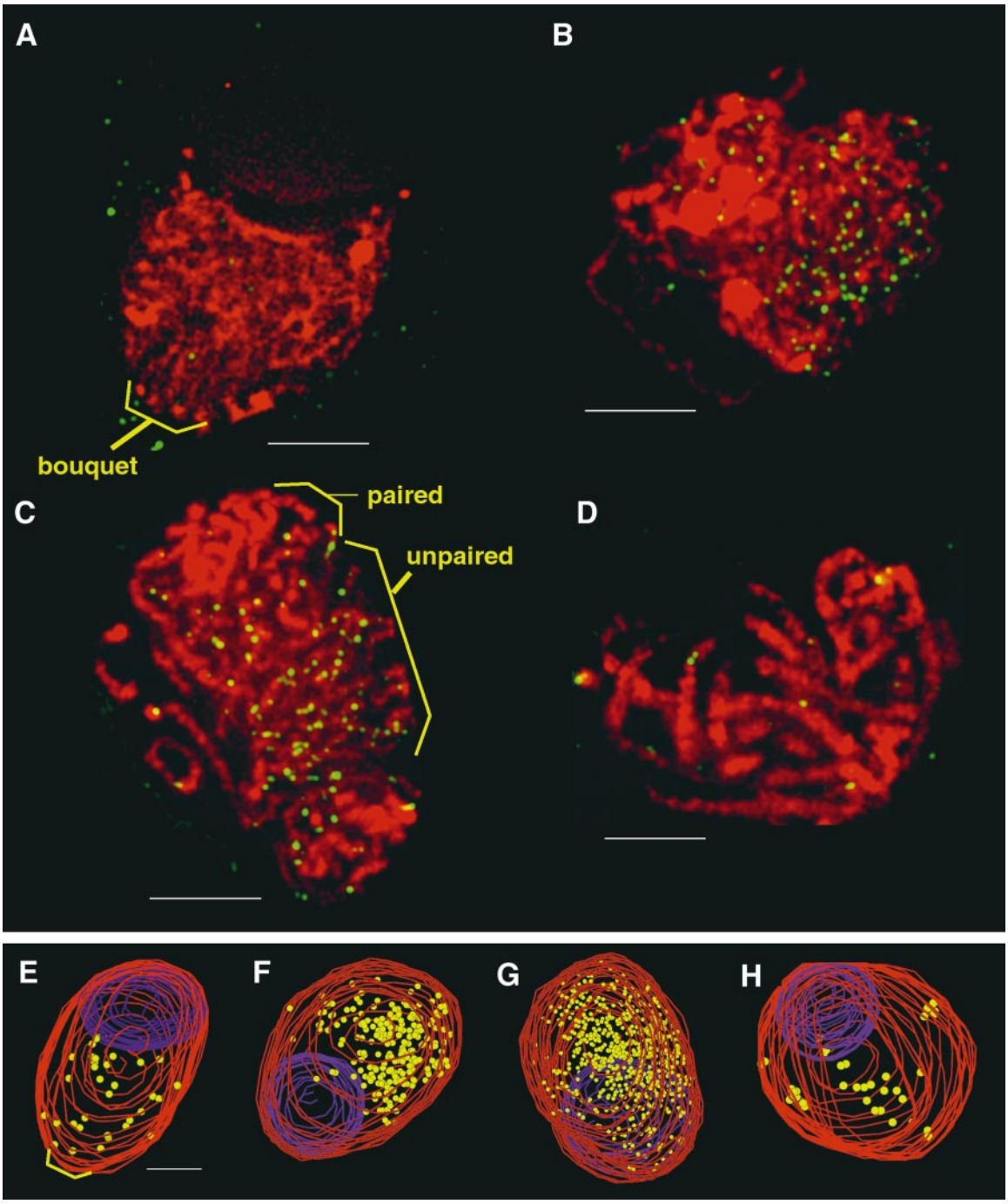

Figure 6. Rad51 Foci Peak during Zygotene.

Bright Rad51 foci appear on chromosomes during zygotene. Successive stages of maize zygotene nuclei were stained for DNA with DAPI (red) and immunostained with anti-HsRad51 antibodies (green). Below are three-dimensional models for each nucleus: red, nuclear periphery; purple, nucleolus; and yellow, Rad51 foci.

(A) and **(E)** Leptotene-to-zygotene transition nucleus, 0.9-μm projection (three optical sections).

(B) and **(F)** Early zygotene nucleus, 1.8-μm projection (six optical sections).

(C) and **(G)** Mid-zygotene nucleus, 1.8-μm projection (six optical sections).

(D) and **(H)** Late zygotene nucleus, 1.8-μm projection (six optical sections).

Bars in **(A)** to **(E)** = 5 μm for **(A)** to **(H)**.

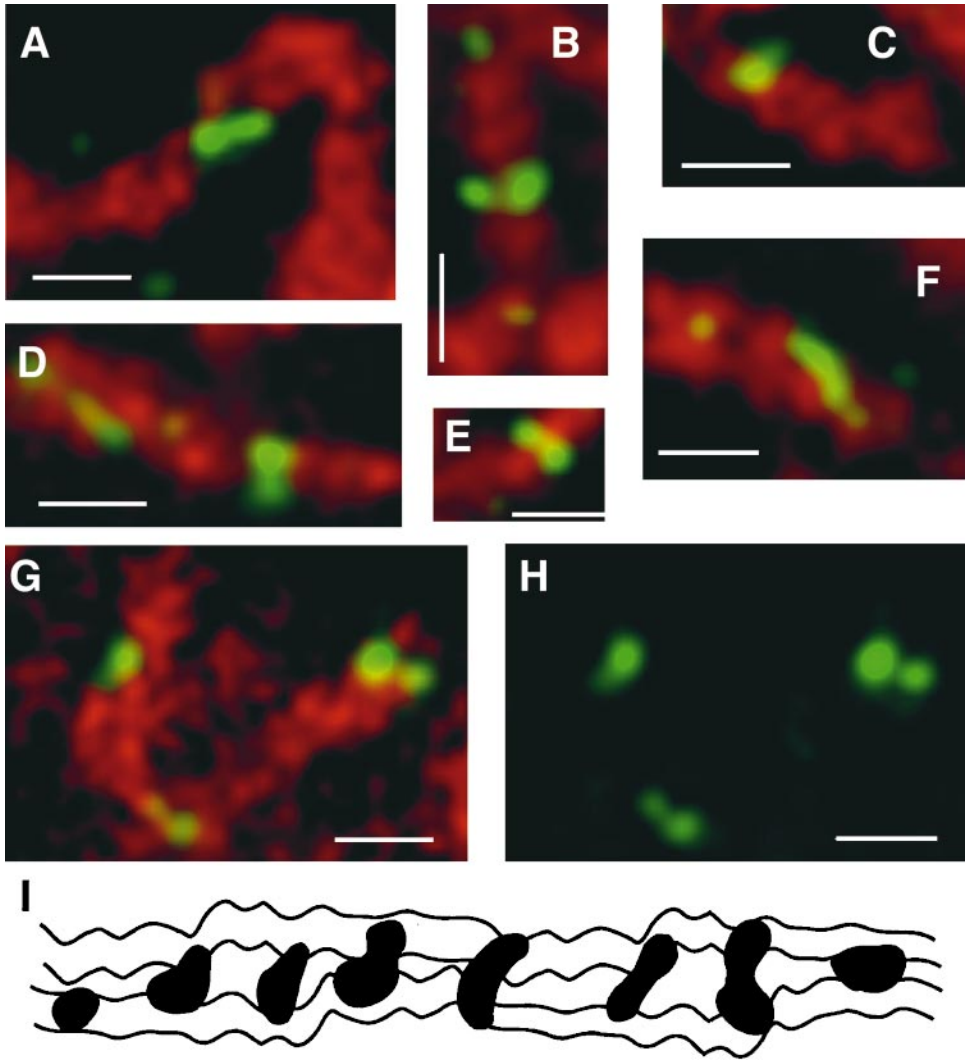

Figure 7. Rad51 Structures on Pairing Chromosomes during Zygotene.

Representative Rad51 paired or bar foci on paired chromosomes from zygotene nuclei stained for DNA with DAPI (red) and immunostained with anti-HsRad51 antibodies (green).
(A) Rad51 structure spanning aligned chromosomes at late zygotene, 2.1-μm projection (seven optical sections).
(B) Paired Rad51 structure and single Rad51 foci on aligned chromosomes at mid-zygotene, 1.5-μm projection (three optical sections).
(C) Comma-shaped Rad51 structure on aligned chromosomes at mid-zygotene, 2-μm projection (four optical sections).
(D) Paired Rad51 structure on aligned chromosomes at mid-zygotene, 1.5-μm projection (five optical sections).
(E) Paired Rad51 structure on aligned chromosomes at mid-zygotene, 1.5-μm projection (three optical sections).
(F) Bar-like Rad51 structure spanning aligned chromosomes at late zygotene, 1.8-μm projection (six optical sections).
(G) and **(H)** A single set of pairing chromosomes with three Rad51 structures on the aligned chromosomes at mid-zygotene, 1.8-μm projection (six optical sections). In **(H)**, only the Rad51 signals are shown.
(I) Cartoon of the variety of Rad51 structures observed during zygotene. The structure at the far right is an identically scaled Rad51 focus from a pachytene nucleus.
Bars in **(A)** to **(H)** = 1 μm.

and the third set has paired Rad51 foci. In Figure 7I, we present the variety of Rad51 structures seen during zygotene from single foci at the far left proceeding to the paired Rad51 structures. For comparison, there is an identically scaled pachytene Rad51 focus. Based on their association with paired chromosomes, it is possible that the paired Rad51 foci are the sites at which chromosome homology is being compared. The different morphologies observed could represent intermediate structures associated with this process.

Rad51 Foci Are Present When Recombination Is Completed

By pachytene, each set of homologous chromosomes is paired along its entire length (Figure 8). The pachytene Rad51 foci generally were larger and brighter than the zygotene Rad51 foci and seemed to lie between the chromosomal axes rather than over them. A significant portion of the Rad51 foci was paired in pachytene, ~25% on average. However, this large number may reflect our inability to discriminate between the end of zygotene and the beginning of pachytene because we do not have markers for the installation of the central SC. Because synapsis is complete at the end of zygotene, whereas recombination is still occurring during pachytene, this means we cannot determine whether these paired foci are completing chromosome pairing or are involved in recombination. However, because one mid-pachytene nucleus had 12 single, unpaired Rad51 foci, this means that paired Rad51 foci are not an obligate feature of pachytene nuclei. In contrast, all zygotene nuclei had significant numbers of paired Rad51 foci (Figure 5).

In the pachytene nuclei, we observed 15 Rad51 foci per nucleus on average (Figure 5), which is less than the expected 20 to 25 homologous recombination events per nucleus (Darlington, 1934). However, Gillies (1983) also observed a lower number of late recombination nodules during pachytene by using serial section electron microscopy (mean = 5; range, 0 to 22 nodules). These late recombination nodules have been correlated directly with chiasmata and meiotic exchange (Maguire and Riess, 1994), and Rad51 has been demonstrated to be involved in meiotic recombination. The observed number and timing of the Rad51 foci during pachytene support our interpretation that these foci may be the actual sites of meiotic recombination and the sites of late recombination nodules.

By diplotene, the chromosomes have begun to desynapse. No Rad51 signals were evident on the chromosomes at this or any later stages (data not shown) despite the presence of abundant levels of full-length Rad51 protein seen in protein extracts (Figure 2).

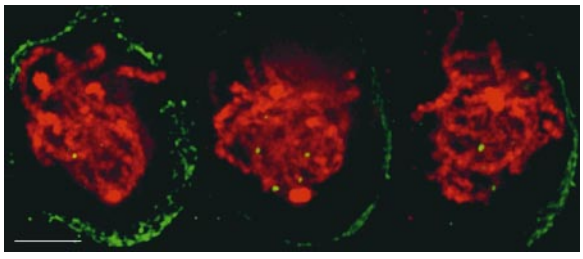

Figure 8. Single Rad51 Foci on Pachytene Chromosomes

Single, bright Rad51 foci are observed on paired chromosomes during pachytene. Shown are three sequential 4.2-μm projections (14 optical sections) from a single pachytene nucleus stained for DNA with DAPI (red) and immunostained with anti-HsRad51 antibodies (green). Bar = 5 μm.

DISCUSSION

We have used three-dimensional molecular cytology to investigate the behavior of Rad51 when chromosomes pair, synapse, and cross over during meiosis in maize. We have found that Rad51 foci develop during zygotene, which is the stage when chromosomes associate and synapse in maize. By using three-dimensional, natively fixed specimens, we have observed that Rad51 first associates with chromosomes coincident with the formation of the telomere bouquet. Furthermore, we have observed and quantified paired Rad51 structures that traverse paired chromosomes. We believe that these are the sites at which the homology comparison takes place. These results lend further support for a role for Rad51 in the chromosomal homology search in addition to its known role in meiotic recombination.

First, we have confirmed that maize, like many other eukaryotes, contains *RAD51* genes, in this case, two closely related versions. Maize is believed to be an ancient allotetraploid, and consequently most of its genes are duplicated (Doebley et al., 1990). Despite their high degree of sequence conservation (90% identity, 94% similarity), ZmRad51a and ZmRad51b proteins are more diverged from each other than the vertebrate Rad51 homologs are among themselves. Nevertheless, ZmRad51a and ZmRad51b appear to be functionally redundant because transposon insertions in either *ZmRAD51* gene do not exhibit a meiotic phenotype (B. Bowen, unpublished data). Double mutant analysis currently is in progress. Neither of these Rad51 proteins represents the maize Dmc1/Lim15 homolog because both nest tightly within the Rad51 subfamily of proteins (Figure 1B; Stassen et al., 1997). Instead, there are two separate *ZmLIM15* genes in maize (S. Tabata, personal communication; J. McElver and B. Bowen, unpublished data). Although both *RAD51* maize genes are expressed at low levels throughout somatic tissues, their transcripts accumulate significantly in tissues about to undergo meiosis. This increase in transcript abundance is

mirrored by the accumulation of protein during meiotic prophase, beginning at leptotene and persisting to the tetrad stage.

Rad51 Appearance Coincides with the Telomere Bouquet

In all organisms examined thus far, Rad51 foci appear early in meiotic prophase; however, the precise substage is not clear. Our data suggest that the large numbers of zygotene Rad51 foci develop during this stage when the telomere bouquet has developed because we see none or very few foci ($n = 10$) in nonbouquet leptotene nuclei and very few foci ($n = 34$) in the early bouquet zygotene transition nucleus. In mice, Plug et al. (1996) observed Rad51 foci beginning at premeiotic S phase, whereas both Moens et al. (1997) and Barlow et al. (1997) saw Rad51 foci appear during leptotene, coincident with the installment of the Cor or SCP3 axial element proteins. Terasawa et al. (1995) observed large numbers of Rad51 foci on unpaired lily chromosomes at a stage described as leptotene. Like maize, both lily meiocytes and mouse spermatogonia form a telomere bouquet (Holm, 1977; Scherthan et al., 1996). Because nuclei were spread for analysis in all previous studies of Rad51 localization during meiosis, polarization of the chromosomes in the nucleus due to the bouquet would be lost. Therefore, from these studies, it is unclear whether Rad51 foci appear before or after the development of the telomere bouquet in mice and lily. From the work by Scherthan et al. (1996), the assembly of the SCP3 axial element protein follows the formation of the telomere bouquet; thus, by inference, in mice the formation of Rad51 foci also may follow the telomere bouquet, as we observed for maize.

Rad51 Foci Are Closely Coordinated with Chromosome Pairing and Synapsis

During zygotene, Rad51 foci were observed on the chromosomes throughout the nucleus in front of the wave of chromosome pairing. Single Rad51 foci were present on both paired and unpaired chromosomes, and paired Rad51 foci were observed on paired chromosomes. As synapsis proceeded through zygotene, the numbers of Rad51 foci rose from 34 to nearly 700 by mid-zygotene and then decreased to <50 by the end of zygotene (Figure 5). This general pattern has been observed in other organisms in which peak numbers of Rad51 foci are associated with the maximum levels of synapsing chromosomes (Moens et al., 1997). The large numbers of Rad51 foci during zygotene in maize ($\sim$500), mice (250), and lily (1000 per mm^2) argue against an exclusive role for Rad51 in meiotic recombination. In maize, there are $\sim$25 recombination events per meiosis, and it would seem both unnecessary and catastrophic to form 500 double-stranded breaks to initiate recombination when only 25 crossovers are formed. It is possible that the other $\sim$475 sites result in gene conversions, but there are no data to support this. Although very little quantitative data exist on meiotic gene conversion in plants, Copenhaver et al. (1998) did not observe any gene conversion events in Arabidopsis, despite scoring >1000 polymorphic loci. Instead, we favor the view that the numerous foci are involved in performing the chromosome homology search just before synapsis during zygotene.

This illustrates another controversy: When is the search for chromosome homology performed? It has been argued that homologous chromosomes are associated before meiosis in organisms such as Drosophila, thereby eliminating the need for a homology search during meiosis. However, Scherthan et al. (1998) have demonstrated that homologous human chromosomes only begin to associate with each other in zygotene. This also appears to be the case for maize. Homologous knob loci in maize (Dawe et al., 1994) and homologous maize chromosomes introgressed into oats (H. Bass, personal communication) are spatially separated and do not associate or coalign until the telomere bouquet forms at the beginning of zygotene. Therefore, in humans, maize, and oats, the chromosome homology search must occur during zygotene, when we observed maximum numbers of Rad51 foci. The controversy still has not been resolved for wheat, because Aragon-Alcaide et al. (1997) have observed the premeiotic pairing of a rye chromosome in a rye/wheat introgression line. In contrast, Hobolth (1981), using serial section electron microscopy with reconstruction, ruled out premeiotic chromosome pairing to account for correct bivalent formation in hexaploid wheat.

Paired Rad51 Foci May Be Sites of the Homology Search

The paired Rad51 foci that we consistently observed in zygotene (Figure 6) may be the sites of DNA sequence comparison and may serve to hold homologs together for synapsis. As mentioned in Results, the paired/contiguous Rad51 foci were observed in both the raw and the deconvolved data, indicating that these structures are not an artifact of the deconvolution process. The maintenance of nuclear and chromatin structure by the special fix and embedding conditions rules out the possibility that these structures are derived from spreading or other damage. Finally, it is unlikely that these paired Rad51 foci on coaligned chromosomes are associated merely by chance because we saw them in late zygotene nuclei, when there are very few Rad51 foci.

Structures resembling the maize Rad51 pairs can be seen on zygotene nuclei; paired Rad51 foci were not evident on synapsed cores of spread chromosomes, but some unsynapsed regions had Rad51 foci at the same sites along the length of both axes (Ashley et al., 1995; Moens et al., 1997). In light of the paired Rad51 foci in maize nuclei, it is tempt-

ing to interpret the equivalently positioned Rad51 foci on opposite axes as originating from paired Rad51 structures that were ripped apart by spreading. In Allium, electron-dense structures similar to paired Rad51 foci can be seen spanning a set of pairing lateral elements that do not yet have a central element installed (Albini and Jones, 1987). These data support the interpretation that paired Rad51 foci structures are present before the installation of the central SC element and may persist to stabilize homologously paired chromosomes while the central element of the SC is being installed.

The paired Rad51 foci appear to be centered over the chromosomal axes with a weaker signal spanning the space between the chromosomes. The molecular nature of this Rad51 structure is not known; however, there are several possibilities. The Rad51 structure could represent accessible portions of a single Rad51/single-stranded DNA monofilament extending between the two chromosomes with the central region protected from antibody staining by a structure, such as an early recombination nodule. Alternatively, the doublet could represent a double Holliday junction (Schwacha and Kleckner, 1995), which would account for the two adjacent foci of the doublet. Regardless of which structure is correct for the adjacent/paired zygotene foci, it must minimally contain 4000 nucleotides within the Rad51 nucleofilament to extend across the maize SC, which is ~200 nm wide. This calculation is based on the fact that Rad51, like RecA, extends the DNA 1.5 times in length (Nishinaka et al., 1998). Because the paired/contiguous zygotene Rad51 foci that span pairing chromosomes have peak intensities 460 nm apart, the minimum DNA associated with this structure would be ~9200 nucleotides. Although this may seem large, only a portion of this structure could be involved in the homology search on the other chromosome because it first needs to traverse the interchromosome space.

Rad51 and Meiotic Recombination during Pachytene

Rad51 is required for meiotic recombination (Shinohara et al., 1992). In maize, ~15 Rad51 foci were observed during pachytene when meiotic recombination is completed, which is less than the ~25 recombination events that occur on average in the maize meiocyte (Darlington, 1934). However, Gillies (1983) also observed fewer recombination nodules than expected in pachytene maize nuclei by using serial section electron microscopy. To account for this difference between the number of recombination nodules and expected recombinations, he suggested that crossovers were formed sequentially on a chromosome. Because the role of Rad51 in meiotic recombination is to initiate DNA strand exchange, once this process has been started, Rad51 may disassemble from that site. This may account for the inability of Anderson et al. (1997) to observe Rad51 staining of late recombination nodules. Because processes such as branch migration and resolution of the Holliday junctions (Dunderdale et al., 1991; Hyde et al., 1994) probably occur during pachytene, these processes could result in the displacement of Rad51 from the DNA. It is not known exactly when the DNA strand transfer associated with meiotic recombination is initiated in maize; however, we favor the view that the Rad51 foci present at pachytene are formed de novo and are not holdovers from zygotene. Nevertheless, our data do not allow us to exclude the possibility that a small subset of the zygotene Rad51 foci persist into pachytene and then develop into the foci associated with the ~25 crossovers typically observed in maize.

A Model for Rad51-Mediated Chromosome Pairing

Based on our observations, we have developed a model to explain the behavior of Rad51 in maize meiocytes during the chromosome homology search (Figures 9A and 9B). At the beginning of zygotene, chromosomes are unpaired. During zygotene, both the chromosome homology search and chromosome synapsis occur at a time when there are peak numbers of Rad51 foci. Although the Rad51 foci seem to be present randomly along the length of unpaired chromosomes, we predict that those foci nearest the telomeres will have the best opportunity to perform a successful homology search and identify partner chromosomes. This would account for the observations that synapsis generally initiates near the telomeres (Burnham et al., 1972).

In contrast to the model of Plug et al. (1996) in which two Rad51 foci, one on each homolog, come together and fuse to catalyze the homology search and synapsis, we suggest in our model that a single Rad51 focus, in the process of performing a homology search on another chromosome, would become a contiguous or paired Rad51 structure. If DNA homology is found, the Rad51 structure would persist and stabilize the paired chromosome while the central element of the SC was being installed. If not, the Rad51 structure should retract and remain inactive until another chromosome comes into proximity. Rad51 structures that may be intermediates in the formation of the paired/contiguous Rad51 structure are presented in a possible temporal sequence in Figure 7I. That all of these forms may be intermediates is supported by the observation that some of them are present on one pairing chromosome. Because few Rad51 foci are found on completely paired chromosomes, synapsis would lead to disassembly of the Rad51 foci as well as inhibiting the reformation of new single Rad51 foci. As the central element of the SC is installed, it would help bring adjacent chromosome segments close enough together, allowing other single Rad51 foci to initiate another round of the homology search. Thus, synapsis would follow the homology search, thereby ensuring the fidelity of chromosome pairing. This model helps to explain how pairing and synapsis can be coupled together in a processive and vectorial manner.

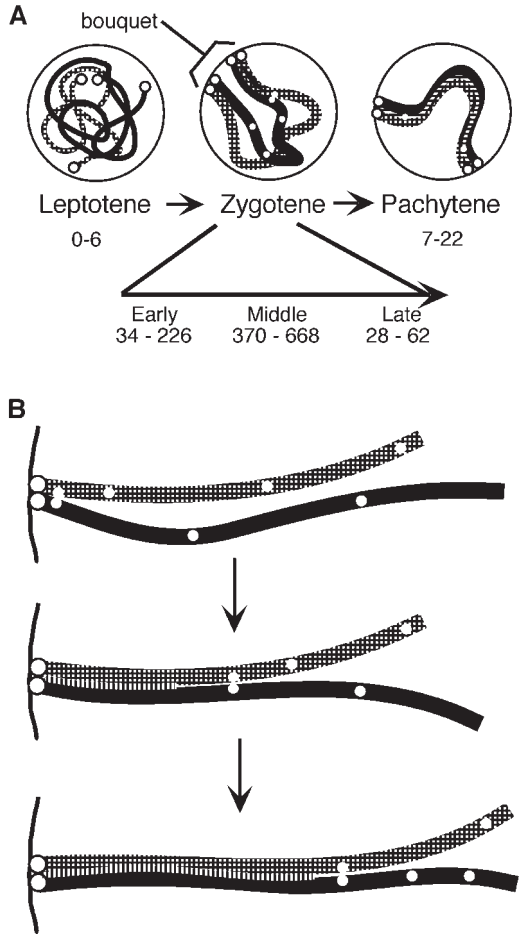

Figure 9. Summary and Model of Rad51 Behavior during Meiotic Prophase.

(A) Summary of Rad51 data superimposed over chromosome behavior. In leptotene, no Rad51 foci are observed, homologous chromosomes (black and cross-hatched) are unpaired, and telomeres (large circles at the chromosome ends) are distributed throughout the nucleus. At the beginning of zygotene, the telomeres attach and cluster, forming the telomere bouquet. At the same time, single Rad51 foci (small unfilled circles) are observed on the chromosomes, and bilobed Rad51 structures are observed on the paired regions of chromosomes as they undergo synapsis. Single Rad51 foci and Rad51 pairs peak in mid-zygotene and then fall off. In pachytene, the telomere bouquet disperses, and a few single Rad51 foci are observed on the synapsed chromosomes.

(B) Model for Rad51 in the chromosome homology search. At the beginning of zygotene, Rad51 foci (small unfilled circles) would appear randomly along the length of the chromosomes. Those foci adjacent to the telomeres (large circles on nuclear envelope) are within close proximity to their homologous chromosomes, and a single Rad51 focus would form a bilobed Rad51 pair in the process of searching the partner chromosome for homology. The Rad51 pairs would stabilize homologously paired chromosomes, and this would allow for the installation of the central element of the SC (vertical hatch marks). As the assembly of the SC proceeded through each Rad51 pair, it would cause its disassembly and inhibit the reinstallation of new Rad51 foci. More distal regions of the homologous chromosomes would then be brought into proximity, which would allow new single Rad51 foci to reinitiate homology comparison by forming the bilobed Rad51 paired structures.

Our model is consistent with observations of Rad51 behavior in other organisms. In yeast, synapsis, as defined by the installation of the SC protein, ZIP1, causes the disappearance of Rad51/Dmc1 complexes (Bishop, 1994). In mice, ~250 Rad51 foci were observed when there was a maximal level of chromosome synapsis. Rad51 foci persisted on the unsynapsed regions of the mouse XY chromosome pair, again suggesting that synapsis during zygotene is necessary to disassemble these foci. Furthermore, these regions do not undergo recombination, indicating that Rad51 foci are not obligatorily associated with meiotic recombination.

It has been suggested that chromosome pairing occurs independently of Rad51 and that chromosome synapsis requires Rad51. This is based on the fact that in *S. cerevisiae*, double-stranded breaks are required for both meiotic recombination and chromosome synapsis, resulting in the interpretation that meiotic recombination is required for synapsis (Weiner and Kleckner, 1994). Consequently, the involvement of RAD51 and DMC1 genes in homologous chromosome pairing and synapsis in yeast was interpreted as a requirement for meiotic recombination to initiate axial association and synapsis of homologous chromosomes (Rockmill et al., 1995). However, in *Bombyx mori* females, Drosophila, and *Caenorhabditis elegans*, homologous chromosomes can pair and synapse without undergoing meiotic recombination (Rasmussen and Holm, 1978; Dernberg et al., 1998; McKim et al., 1998). This indicates that meiotic recombination can be uncoupled from chromosome synapsis in these organisms. In maize, both the homology search and synapsis occur during zygotene, precluding the possibility of premeiotic chromosome pairing. Furthermore, maize only undergoes ~25 meiotic recombinations per nucleus, whereas there are an average of 500 Rad51 foci during zygotene. Taken together, these observations support a separate role for Rad51 in the chromosome homology search.

By establishing a complete description of Rad51 behavior in normal maize meiosis, we now can ask whether any of the maize chromosome pairing mutants exhibit aberrant patterns of Rad51 localization during zygotene. Aberrant synapsis of chromosomes recently has been observed in meiocytes from Dmc1 gene knockout mice (Yoshida et al., 1998), indicating that this Rad51 homolog is required for homologous chromosome synapsis. By combining molecular cytology with mutant analysis in an organism amenable to cytological analysis, we should be able to integrate our knowledge of the molecular events of meiosis with these large-scale meiotic events in the nucleus.

METHODS

Plant Material and Fixation

Maize (*Zea mays*) inbred strains A344, A665, and W23 were grown in the greenhouse, and immature tassels were harvested before emergence. Anthers 0.8 to 2.5 mm in length containing meiocytes from leptotene to pachytene/diplotene were dissected from the tassel florets and fixed for 30 to 45 min, essentially according to Dawe et al. (1994), modified by including 0.05% Tween 20 in 4% formaldehyde–buffer A (15 mM Pipes [Boehringer Mannheim], pH 7.0, 80 mM KCl, 20 mM NaCl, 2 mM EDTA, 0.5 mM EGTA, 0.2 mM spermine, 0.5 mM spermidine, 1 mM DTT, and 0.32 M sorbitol). Anthers were rotated in a 1.5-mL Eppendorf tube in the fixative followed by two 1-hr washes with buffer A. Meiocytes were extruded carefully from cut anthers and embedded in a 5% polyacrylamide pad, as previously described (Bass et al., 1997), on a cover slip by using 3M Magic tape (3M, St. Paul, MN) as spacers (63 μm depth).

Cloning and Characterization of *ZmRAD51a* and *ZmRAD51b*

Polyadenylated mRNA was prepared from different tissues of maize inbred A632 by using the MicroQuick kit (Pharmacia), and standard methods for hybridization, cDNA synthesis, and cloning were used (Sambrook et al., 1989). Initially, a 360-bp fragment derived from *ZmRAD51a* was obtained using polymerase chain reaction with first-strand cDNA made from tassel mRNA and a set of degenerate primers derived from *RAD51* consensus sequences. This cloned fragment was labeled with digoxigenin by using the Genius kit (Boehringer Mannheim) and used as a probe to screen a commercially prepared λ Zap library (Stratagene, La Jolla, CA) made from tassel mRNA prepared from maize inbred A632. Two classes of cDNA clones were isolated, and the sequences of the predominant *ZmRAD51a* and *ZmRAD51b* cDNAs with the longest 3′ untranslated regions were determined. They have GenBank accession numbers AF079428 and AF079429. Full-length cDNA clones for each gene (*PHP7981* and *PHP7983*) are available upon request. To facilitate subcloning of the *ZmRAD51a* and *ZmRAD51b* coding sequences for expression studies, we introduced a BamHI site immediately upstream of the start codon, and a HpaI site was introduced immediately downstream from the stop codon of each gene by site-specific mutagenesis. The 3′ untranslated regions from the HpaI-modified genes were used as gene-specific probes. The *ZmRAD51a* and *ZmRAD51b* genes were mapped using a propietary F_2 restriction fragment length polymorphism mapping population.

Protein Gel Blot Analysis

The *ZmRAD51a* cDNA was subcloned into the *Escherichia coli* expression vectors pQE30 (Qiagen, Chatsworth, CA) to generate a fusion protein with an N-terminal six-histidine tag that was purified on Talon resin (Clontech, Palo Alto, CA) and injected into rabbits for antibody production. SDS-PAGE was performed using purified His_6-ZmRad51a protein, meiotic tassel extracts, and sized anthers (both from maize inbred A344) chopped up in 20 mL of 1 × SDS-PAGE sample buffer with 8 M urea (Harlow and Lane, 1988). Electrophoretic transfer of protein to polyvinylidene difluoride or nitrocellulose membranes was followed by incubation with anti-HsRad51 (at 1:500; Terasawa et al., 1995) or ZmRad51a (at 1:1000) antibodies and then by incubation with anti–rabbit antibodies conjugated with horseradish peroxidase (at 1:5000; Jackson ImmunoResearch, West Grove, PA) and chemiluminescence ECL reagent (Amersham) to visualize protein bands.

Immunofluorescence

Fixation and embedding procedures previously shown to maintain both native chromatin structure (Dawe et al., 1994) and the three-dimensional architecture of the nucleus (Bass et al., 1997) were followed so that stage-specific changes in chromatin and nuclear architecture could be used to precisely establish the meiotic substage of the cell. The conditions for three-dimensional immunofluorescence were first determined using a monoclonal antibody specific for histone H1. Complete nuclear staining by the antibodies and low background noise were achieved by performing antibody incubations and washes overnight. Chromosomal morphology after histone H1 staining was identical to that observed after 4′,6-diamidino-2-phenylindole (DAPI) staining of the same nucleus (data not shown) and was similar to that described previously by Dawe et al. (1994).

The cover slips with the polyacrylamide pads containing the fixed meiocytes were incubated in 1 × PBS twice for 10 min to leach out the polymerization catalysts. Subsequently, cells were permeabilized for 30 min to 1 hr in 1 × PBS, 1% Triton X-100, and 1 mM EDTA and then blocked for 1 hr in 1 × PBS, 3% BSA, 5% normal donkey serum, 1 mM EDTA, and 0.1% Tween 20. Samples were incubated overnight in a humid chamber with 50 mL of a 1:500 dilution of the anti-HsRad51 antibody (Terasawa et al., 1995) precleared for 30 min at 4°C with *E. coli* XL1-Blue acetone powder in blocking buffer. After 24 hr, samples were washed five to eight times, 1 hr for each wash, in 1 × PBS, 0.1% Tween 20, and 1 mM EDTA, with continued washing overnight in a humid chamber. A fluorescein isothiocyanate–labeled donkey anti–rabbit $(Fab')_2$ fragment (Jackson ImmunoResearch) at 1 mg/mL in blocking buffer was incubated overnight, and the identical washing protocol was followed the next day and night. Samples were stained with 10 mg/mL DAPI for 1 hr followed by two 1-mL washes of 1 × PBS, transferred into 5% Tris (from 2 M Tris base) and 95% glycerol (Omni-Solv; EM Science, Gibbstown, NJ) containing 2% *n*-propyl gallate (Giloh and Sedat, 1982), and then sealed with clear fingernail polish and stored at −20°C.

Microscopy

All images were obtained using an Olympus (Lake Success, NY) IMT-2 wide-field fluorescence microscope with an oil immersion ×60 Plan-Apo lens, N.A. 1.4, combined with a ×1.5 relay lens. To generate an axially symmetric point–spread function to minimize spherical aberration, we used a high refractive index immersion oil of $\eta = 1.5351$ (Cargille Laboratories, Cedar Grove, NJ) to compensate for the low refractive index of the glycerol-based mount ($\eta = 1.4615$). A computer-controlled stage was used to collect 80 to 100 optical sections per nucleus, 300 or 500 nm apart. The optical data were collected using a cooled 12-bit CCD camera. The three-dimensional data sets were first normalized for photobleaching and then processed by 15 iterative deconvolution cycles (Chen et al., 1995).

Image Analysis

The optical sections were collected and analyzed using the software system Resolve3D and Prism (Applied Precision, Inc., Seattle, WA). Maximum intensity projections of three-dimensional data were used when presenting the combined information from successive optical sections. Nuclear Rad51 foci were located automatically in the data sets by identifying local peak intensities in three dimensions. Only those foci that were clearly above background and within the nucleus were counted as Rad51 foci. Paired Rad51 structures were defined as two adjacent or touching foci that were clearly on coaligned chromosomes. Approximately half of the paired/bar Rad51 foci fulfilled these criteria. The Rad51 pairs were not included if the two chromosome axes were not clearly distinguishable or coaligned, for example, perpendicular to each other. This was particularly difficult in early and mid-zygotene nuclei, which have dense tangles of chromosomes. In addition, if foci were paired in the axial direction, they could not be counted due to the lower resolution in the z axis (500 nm). Based on these strict criteria in addition to optical limitations, the number of paired Rad51 foci per nucleus may have been underestimated by half.

ACKNOWLEDGMENTS

We thank John Sedat and David Agard (University of California, San Francisco) for training and access to their deconvolution microscope system and for helpful comments on the manuscript. We thank Tomoko Ogawa (National Institute of Genetics, Mishima, Japan) for the generous gift of the HsRad51 antibodies and Dr. Alan Epstein (University of Southern California, Los Angeles) for the gift of monoclonal histone H1 antibody. We especially thank Hank Bass and Lisa Harper and former and current members of the Sedat and Cande laboratories for invaluable help with microscopy, image analysis, and stimulating discussions. We thank Jan Paluh and Lisa Harper for their comments on the manuscript. W.Z.C. and A.E.F. were supported by National Institutes of Health Grant No. RO1 GM48547. A.E.F. was also supported by a National Institutes of Health postdoctoral fellowship, and R.R. was supported by a grant from Pioneer Hi-Bred International, Inc.

Received October 19, 1999; accepted February 18, 1999.

REFERENCES

Albini, S.M., and Jones, G.H. (1987). Synaptonemal complex spreading in *Allium cepa* and *A. fistulosum.* Chromosoma **95,** 324–338.

Anderson, L.K., Offenberg, H.H., Verkuijlen, W.M.H.C., and Heyting, C. (1997). RecA-like proteins are components of early meiotic nodules in lily. Proc. Natl. Acad. Sci. USA **94,** 6868–6873.

Aragon-Alcaide, L., Reader, S., Beven, A., Shaw, P., Miller, T., and Moore, G. (1997). Association of homologous chromosomes during floral development. Curr. Biol. **7,** 905–908.

Ashley, T., Plug, A.W., Xu, J., Solari, A.J., Reddy, G., Golub, E.I., and Ward, D.C. (1995). Dynamic changes in Rad51 distribution on chromatin during meiosis in male and female vertebrates. Chromosoma **104,** 19–28.

Barlow, A.L., Benson, F.E., West, S.C., and Hulten, M.A. (1997). Distribution of the RAD51 recombinase in human and mouse spermatocytes. EMBO J. **16,** 5207–5215.

Bass, H.W., Marshall, W.F., Sedat, J.W., Agard, D.A., and Cande, W.Z. (1997). Telomeres cluster *de novo* before the initiation of synapsis: A three-dimensional spatial analysis of telomere positions before and during meiotic prophase. J. Cell Biol. **137,** 5–18.

Baumann, P., Benson, F.E., and West, S.C. (1996). Human Rad51 protein promotes ATP-dependent homologous pairing and strand transfer reactions in vitro. Cell **87,** 757–766.

Benson, F.E., Baumann, P., and West, S.C. (1998). Synergistic actions of Rad51 and Rad52 in recombination and DNA repair. Nature **391,** 401–404.

Bishop, D.K. (1994). RecA homologs Dmc1 and Rad51 interact to form multiple nuclear complexes prior to meiotic chromosome synapsis. Cell **79,** 1081–1092.

Bishop, D.K., Park, D., Xu, L., and Kleckner, N. (1992). *DMC1*: A meiosis-specific yeast homolog of E. coli *recA* required for recombination, synaptonemal complex formation, and cell cycle progression. Cell **69,** 439–456.

Burnham, C.R., Stout, J.T., Weinheimer, W.H., Knowles, R.V., and Phillips, R.L. (1972). Chromosome pairing in maize. Genetics **71,** 111–126.

Carpenter, A.T.C. (1975). Electron microscopy of meiosis in *Drosophila melanogaster* females. I. Structure, arrangement, and temporal change of the synaptonemal complex in wild-type. Chromosoma **51,** 157–182.

Chen, H., Swedlow, J.R., Grote, M.A., Sedat, J.W., and Agard, D.A. (1995). The collection, processing, and display of digital three-dimensional images of biological specimens. In Handbook of Biological Confocal Microscopy, J. Pawley, ed (New York: Plenum Press), pp. 197–210.

Cheng, R., Baker, T.I., Cords, C.E., and Radloff, R.J. (1993). Mei-3, a recombination and repair gene of *Neurospora crassa*, encodes a RecA-like protein. Mutat. Res. **294,** 223–234.

Copenhaver, G.P, Browne, W.E., and Preuss, D. (1998). Assaying genome-wide recombination and centromere functions with *Arabidopsis* tetrads. Proc. Natl. Acad. Sci. USA **95,** 247–252.

Creighton, H.B., and McClintock, B. (1931). A correlation of cytological and genetical crossing over in *Zea mays.* Proc. Natl. Acad. Sci. USA **17,** 492–497.

Darlington, C.D. (1934). The origin and behavior of chiasmata. VII. *Zea mays.* Z. Indukt. Abstammungs Vererbungsl. **67,** 96–114.

Dawe, R.K., Sedat, J.W., Agard, D.A., and Cande, W.Z. (1994). Meiotic chromosome pairing in maize is associated with a novel chromatin organization. Cell **76,** 901–912.

Dernburg, A.F., Sedat, J.W., Cande, W.Z., and Bass, H.W. (1995). Cytology of telomeres. In Telomeres, E.H. Blackburn and C.W. Grieder, eds (Cold Spring Harbor, NY: Cold Spring Harbor Laboratory Press), pp. 295–338.

Dernberg, A.F., McDonald, K., Moulder, G., Barstead, R., Dresser, M., and Villanueve, A. (1998). Meiotic recombination in C. elegans initiates by a conserved mechanism and is dispensible for homologous chromosome synapsis. Cell **94,** 387–398.

Doebley, J., Stec, A., Wendel, J., and Edwards, M. (1990). Genetic and morphological analysis of a maize-teosinte F2 population:

Implications for the origin of maize. Proc. Natl. Acad. Sci. USA **87,** 9888–9892.

Dunderdale, H.J., Benson, F.E., Parsons, C.A., Sharples, G.J., Lloyd, R.G., and West, S.C. (1991). Formation and resolution of recombination intermediates by *Escherichia coli* RecA and RuvC proteins. Nature **354,** 506–510.

Gillies, C.B. (1975). An ultrastructural analysis of chromosomal pairing in maize. Carlsberg Res. Commun. **40,** 135–162.

Gillies, C.B. (1983). Ultrastructural studies of the association of homologous and non-homologous parts of chromosomes in the mid-prophase of meiosis in *Zea mays.* Maydica **28,** 265–287.

Giloh, H., and Sedat, J. (1982). Fluorescence microscopy: Reduced photobleaching of rhodamine and fluorescein protein conjugates by *n*-propyl gallate. Science **217,** 1252–1255.

Gupta, R.C., Bazemore, L.R., Golub, E.I., and Radding, C.M. (1997). Activities of human recombination protein Rad51. Proc. Natl. Acad. Sci. USA **94,** 463–468.

Harlow, E., and Lane, D. (1988). Antibodies: A Laboratory Manual. (Cold Spring Harbor, NY: Cold Spring Harbor Laboratory Press).

Hobolth, P. (1981). Chromosome pairing in allohexaploid wheat var. Chinese spring. Transformation of multivalents into bivalents, a mechanism for exclusive bivalent formation. Carlsberg Res. Commun. **46,** 129–173.

Holm, P.B. (1977). Three-dimensional reconstruction of chromosome pairing during the zygotene stage of meiosis in *Lilium longiflorum* (Thunb.). Carlsberg Res. Commun. **42,** 103–151.

Hyde, H., Davies, A.A., Benson, F.E., and West, S.C. (1994). Resolution of recombination intermediates by a mammalian activity functionally analogous to *Escherichi coli* RuvC resolvase. J. Biol. Chem. **269,** 5202–5209.

John, B. (1990). Meiosis. (New York: Cambridge University Press).

Maeshima, K., Morimatsu, K., and Horii, T. (1996). Purification and characterization of XRad51.1 protein, Xenopus RAD51 homolog: Recombinant XRad51.1 promotes strand exchange reaction. Genes Cells **1,** 1057–1068.

Maguire, M.P., and Riess, R.W. (1994). The relationship of homologous synapsis and crossing over in a maize inversion. Genetics **137,** 281–288.

Maguire, M.P., Riess, R.W., and Paredes, A.M. (1993). Evidence from a maize desynaptic mutant points to a probable role of synaptonemal complex central region components in provision for subsequent chiasma maintenance. Genome **36,** 797–807.

McKim, K.S., Green-Marroquin, B.L., Sekelsky, J.J., Chin, G., Steinberg, C., Khodosh, R., and Hawley, R.S. (1998). Meiotic synapsis in the absence of recombination. Science **279,** 876–878.

Moens, P.B., Chen, D.J., Shen, Z., Kolas, N., Tarsounas, M., and Heng, H. (1997). Rad51 immunocytology in rat and mouse spermatocytes and oocytes. Chromosoma **106,** 207–215.

Morita, T., Yoshimura, Y., Yamamoto, A., Murata, K., Mori, M., Yamamoto, H., and Matsushiro, A. (1993). A mouse homolog of the *Escherichia coli* RecA and *Saccharomyces cerevisiae* Rad51 genes. Proc. Natl. Acad. Sci. USA **90,** 6577–6580.

Moses, M.J. (1956). Chromosomal structures in crayfish spermatocytes. J. Biophys. Biochem. Cytol. **2,** 215–218.

New, J.H., Sugiyama, T., Zaitseva, E., and Kowalczykowski, S.C. (1998). Rad52 protein stimulates DNA strand exchange by Rad51 and replication protein A. Nature **391,** 407–410.

Nishinaka, T., Shinohara, A., Ito, Y., Yokoyama, S., and Shibata, T. (1998). Base pair switching by interconversion of sugar puckers in DNA extended by proteins of RecA-family: A model for homology search in homologous recombination. Proc. Natl. Acad. Sci. USA **95,** 11071–11076.

Padmore, R., Cao, L., and Kleckner, N. (1991). Temporal comparison of recombination and synaptonemal complex formation during meiosis in *Saccharomyces cerevisiae.* Cell **66,** 1239–1256.

Plug, A.W., Xu, J., Reddy, G., Golbu, E.I., and Ashley, T. (1996). Presynaptic association of Rad51 protein with selected sites in meiotic chromatin. Proc. Natl. Acad. Sci. USA **93,** 5920–5924.

Rasmussen, S.W., and Holm, P.B. (1978). Chromosome pairing in autotetraploid *Bombyx* females. Mechanism for exclusive bivalent formation. Carlsberg Res. Commun. **44,** 101–125.

Rockmill, B., Sym, M., Scherthan, H., and Roeder, G.S. (1995). Roles for two RecA homologs in promoting meiotic chromosome synapsis. Genes Dev. **9,** 2684–2695.

Roeder, G.S. (1995). Sex and the single cell: Meiosis in yeast. Proc. Natl. Acad. Sci. USA **92,** 10450–10456.

Sambrook, J., Fritsch, E.F., and Maniatis, T. (1989). Molecular Cloning: A Laboratory Manual. (Cold Spring Harbor, NY: Cold Spring Harbor Laboratory Press).

Scherthan, H., Weich, S., Schwegler, H., Heyting, C., Haerle, M., and Cremer, T. (1996). Centromere and telomere movements during early meiotic prophase of mouse and man are associated with the onset of chromosome pairing. J. Cell Biol. **134,** 1109–1125.

Scherthan, H., Eils, R., Trelles-Stricken, E., Dietzel, S., Cremer, T., Walt, H., and Jauch, A. (1998). Aspects of three-dimensional chromosome reorganization during the onset of human male meiotic prophase. J. Cell Sci. **111,** 2337–2351.

Schwacha, A., and Kleckner, N. (1995). Identification of double Holliday junctions as intermediates in meiotic recombination. Cell **83,** 783–791.

Shinohara, A., and Ogawa, T. (1998). Stimulation by Rad52 of yeast Rad51-mediated recombination. Nature **391,** 404–407.

Shinohara, A., Ogawa, H., and Ogawa, T. (1992). Rad51 protein involved in repair and recombination in Saccharomyces cerevisiae is a RecA-like protein. Cell **69,** 457–470.

Shinohara, A., Ogawa, H., Matsuda, Y., Ushio, N., Ikeo, K., and Ogawa, T. (1993). Cloning of human, mouse and fission yeast recombination genes homologous to RAD51 and RecA. Nat. Genet. **4,** 239–243.

Smith, K.N., and Nicholas, A. (1998). Recombination at work for meiosis. Curr. Opin. Genet. Dev. **8,** 200–211.

Staiger, C.J., and Cande, W.Z. (1993). Cytoskeletal analysis of maize meiotic mutants. In Molecular and Cell Biology of the Plant Cell Cycle, J. Ormrod and E. Francis, eds (Dordrecht, The Netherlands: Kluwer Academic Publishers), pp. 157–170.

Stassen, N.Y., Logsdon, J.M., Jr., Vora, G.J., Offenberg, H.H., Palmer, J.D., and Zolan, M.E. (1997). Isolation and characterization of Rad51 orthologs from *Coprinus cinereus* and *Lycopersicon*

esculentum, and phylogenetic analysis of eukaryotic *recA* homologs. Curr. Genet. **31,** 144–157.

Stern, C. (1931). Zytologisch-genetische untersuchungen als beweise fur die Morgansche theorie des faktoraustauschs. Biol. Zentbl. **51,** 547–587.

Sung, P. (1997). Function of yeast Rad52 protein as a mediator between replication protein A and the Rad51 recombinase. J. Biol. Chem. **272,** 28194–28197.

Sung, P., and Robberson, D.L. (1995). DNA strand exchange mediated by a RAD51-ssDNA nucleoprotein filament with polarity opposite to that of RecA. Cell **82,** 453–461.

Terasawa, M., Shinohara, A., Hotta, Y., Ogawa, H., and Ogawa, T. (1995). Localization of RecA-like recombination proteins on chromosomes of the lily at various meiotic stages. Genes Dev. **9,** 925–934.

Weiner, B.M., and Kleckner, N. (1994). Chromosome pairing via multiple interstitial interactions before and during meiosis in yeast. Cell **77,** 977–991.

Yoshida, K., Kondoh, G., Matsuda, Y., Habu, T., Nishimune, Y., and Morita, T. (1998). The mouse RecA-like gene Dmc1 is required for homologous chromosome synapsis during meiosis. Mol. Cell **1,** 707–718.